Supporting Information

Ultrathin Planar Graphene Supercapacitors

Jung Joon Yoo,[†,‡,a] Kaushik Balakrishnan,[†,a] Jingsong Huang,[⊥] Vincent Meunier,[⊥,≠,] * Bobby G. Sumpter,[⊥] Anchal Srivastava,[†,‖] Michelle Conway,[†] Arava Leela Mohan Reddy,[†] Jin Yu,[‡] Robert Vajtai,[†] and Pulickel M. Ajayan[†,] *

[†] Mechanical Engineering and Material Science Department, Rice University, Houston, TX, USA, [‡]Department of Material Science and Engineering, KAIST, Daejeon, Republic of Korea, [⊥]Oak Ridge National Laboratory, Oak Ridge, TN, USA, [‖]Department of Physics, Banaras Hindu University, Varanasi, India. [≠]Present address Department of Physics, Applied Physics and Astronomy, Rensselaer Polytechnic Institute, 110 Eighth Street, Troy, New York 12180-3590 USA. [a]These authors contributed equally to this work.

AUTHOR EMAIL ADDRESS ajayan@rice.edu; meuniv@rpi.edu

Table of Contents

1) Materials and Methods

Fabrication and characterization of Pristine Graphene (G). A CVD method based on use of liquid precursor was adopted to realize high-quality G films on Cu-substrate[1]. This film was subsequently transferred to quartz substrate for the final fabrication of the supercapacitor device (see below for the fabrication of supercapacitor devices). The as-grown and transferred G film had area coverage of ~1cm^2. A typical image of the transferred pristine graphene film onto SiO$_2$ substrate is shown in **Figure 2c**.

Fabrication and characterization of Multi-layer Reduced Graphene Oxide (RMGO). A layer-by-layer (LBL) method was first used to create MGO films which were then subsequently chemically reduced by hydrazine to form RMGO films. The electrostatic interactions between the cationic polymer and graphene oxide (GO) allows for creating multi-layer graphene oxide (MGO) films. To this end, two separate aqueous solutions of the polymer and GO were prepared. The cationic polymer, poly (ethyleneimine) (PEI) purchased from Sigma-Aldrich (branched PEI: M$_w$ 25,000), and GO was synthesized from graphite powder (SP-1, Bay Carbon, MI) using the modified Hummers method. The aqueous solutions had concentration of 1 wt% for the PEI and 0.02 wt% for GO. **Note:** During the preparation of the 0.02 wt% GO solution, the GO powder was first dispersed in the required amount of water and sonicated in the water bath. During the sonication process care was taken to keep the temperature below 50 ^{o}C to ensure homogeneity of GO solution.

In a typical LBL process, freshly cleaned quartz slides (TED PELLA, INC.) was immersed first in a 1 wt% PEI solution for 15 min. and rinsed with deionized water followed by drying in air. Then, this polymer treated quartz slide was then immersed in a 0.02 wt% GO solution for 15 minutes to allow for sufficient interactions amongst the polymer and the GO. Following the rinsing with deionized water and drying the quartz slide, the PEI-GO film was again subjected to the same process two more time. Thus, the MGO films were formed by three cycles of dipping and drying. A schematic representation of the LBL process is shown in **Supplementary Fig. S2.** The controlled dipping and drying to yield high quality MGO films were performed using a robot controlled arm on a printing instrument (Asymetek). The film MGO film area was ~2 cm^2. The conversion of the MGO films to RMGO was performed using chemical reduction using hydrazine (N$_2$H$_2$). Before carrying out the chemical reduction, the MGO films comprised of the PEI and GO was subjected to heat-treatment at 350 ^{o}C for 1 h for the removal of the polymer. The heat-treated films were then immersed in a glass bottle containing 0.1 wt% aqueous solution of hydrazine hydrate (64 %, Acros). The bottle was subsequently immersed in an oil bath at 50 ^{o}C for 30 min. The films are then allowed to dry overnight in a fume hood. The color of the films shows a dramatic change following the reduction. The MGO films have a brownish appearance while the final RMGO films show blackish appearance. No change in the overall area of the RMGO film in comparison to the original MGO film is recorded. The two sets of slides before and after reduction are shown in **Fig. 2d**. The mass of the RMGO samples were measured using

CAHN C-31 microbalance (Cahn Instruments, Inc., Cerritos, CA). The SEM images were taken on a field emission scanning electron microscope (FEI Quanta 400 ESEM FEG). The thickness and the general morphology of the RMGO films were performed using AFM (Digital Instrument Nanoscope IIIA). Raman spectroscopic measurements were performed using a Renishaw InVia Raman microscope equipped with a 50x objective lens and a 514.5 nm laser beam.

Fabrication of graphene based supercapacitor devices. A schematic depiction of the device fabrication is shown in **Supplementary Fig. S3**. The total width of the G and RMGO films was reduced to 2 mm using a sharp razor blade which allows for removal of the materials from the pre-fabricated large area. The dimensions of the devices was therefore reduced to 2mm (wide) and 20 mm (long) Gold (current collector) was then sputtered on the edges of the G and RMGO films. A home-made mask was used to cover the active area of the G and RMGO films so that no gold gets deposited over the active area of the device. Then, carefully a scratch was made in the central portion of the G and RMGO film using a sharp razor blade so as to create a gap. This scratch now allows for the formation of the two electrodes comprised of G and RMGO, respectively. To ensure that the two electrodes are completely isolated electrical resistance was measured both before and after the scratch. Indeed, it was found that a single scratch could now allow for the isolation of the two electrodes. The large increase in the resistance of the films from a few kΩ (before scratch) to no measureable resistance (after scratch) provides a direct evidence of the isolation. Moreover, we also observed the scratches made using optical microscope. Typically, the scratches made were ~60 μm wide. Following the isolation of the two electrodes the polymer gel electrolyte was applied across the active electrode surface and the micron-sized gap to create an electrical double layer, which allows for charge separation and mobility (of the ions) across the two electrodes (**Fig. 2a, and Fig. S3, S.I.**). During this step, care is taken to ensure no spreading of the electrolyte occurs on the current collectors. The device is then left overnight in the fume hood for the drying and aging of the polymer gel electrolyte. The polymer gel electrolyte used here is a mixture of poly (vinyl alcohol) (PVA, M_w 85,000-124,000, 99+% hydrolyzed, Aldrich) and phosphoric acid (H_3PO_4). The preparation procedure of PVA–H_3PO_4 electrolyte is described elsewhere[2]. The devices, after complete drying, were then subjected to electrochemical measurements for the evaluation of their supercapacitor behavior. A typical 2D in-plane device used for evaluating electrochemical supercapacitor performance is shown in **Fig. 2a**.

Electrochemical Characterization. The cyclic voltammetry (CV) and galvanostatic charge-discharge measurement was done using both AUTOLAB PGSTAT 302N and Princeton Applied Research Bistat using two electrode system. The CVs were tested at various scan rates from 1-100 mVs^{-1} in the range of 0 to 1 V. Galvanostatic charge-discharge curves were obtained using a suitable constant current density for each device. EIS measurements were carried out at a dc bias of 0 V with sinusoidal signal of 100 mV over the frequency range from 20 kHz to 10 mHz.
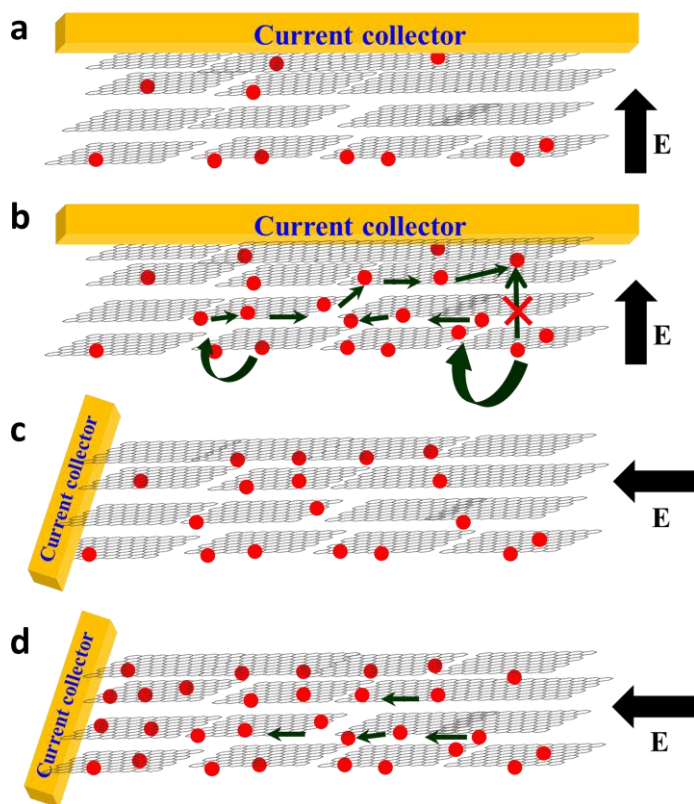
2) Supporting Figures

Figure S1. Schematic depiction for the performance comparison of the conventional stacked geometry (a,b) Vs the 'in-plane' geometry (c,d). The illustration is depicted only for a single electrode (as the situation is expected to be the same in the electrode as well). As shown in the figure, the graphene films are comprised of graphene flakes, which are well connected with sufficient porosity to enable the complete coverage of the electrode surface by the electrolyte ions. Given that the nature of the electrode and electrolyte remains unchanged in both the geometries, upon reaching an equilibrium the capacity should be same, independent of the geometry. Upon charging, the initial ions created in the conventional stacked geometry can start to populate certain regions (as shown in a). For these charges to now move across the electrode surface with the applied electric field, to populate different regions of the offered electrochemical area from the electrode the ions will need to overcome the barrier from the flakes, driven by the electric field (which is now perpendicular to the electrode surface) to cross over the sheets to penetrate into the electrode material (as shown in b). The movements of the ions are favored along the planar graphene sheet rather than perpendicular to it, owing to the nature of graphene. Furthermore, as more like ions cross over from the other electrode, the situation becomes more complex, as the electrolyte ions need to additionally cross the barrier (shown before) to populate the electrode surface. If the charging is allowed to reach equilibrium then indeed one should observe the same capacity, again regardless of the geometry. In comparison, the initial charges formed in the case of 'in-plane' device geometry (as shown in c) can fill in (or move) more rapidly as the electric field is in the same direction of the organized electrode materials composed of multi-layer graphene (as shown in d), and therefore offer increased specific capacity for the same amount of area despite the fact that the ions need to travel a larger distance (length of the electrode, ~ 100 mm) in the 'in-plane' configuration as opposed to those in case of the stacked geometry (from a few nm to upto a few mm). As supercapacitor devices are operated far from equilibrium the 'in-plane' graphene devices offers better charge mobility along with effective utilization of the electrochemical surface area as opposed to the conventional stacked device geometry.
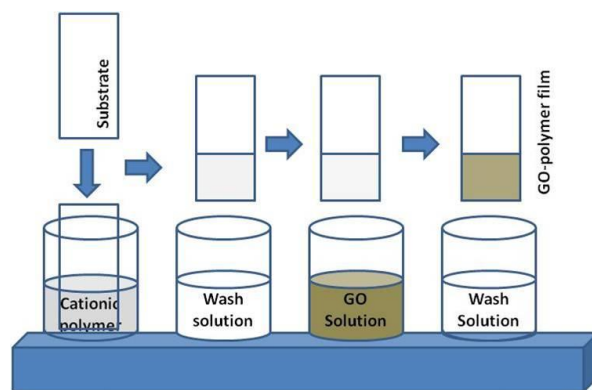
Figure S2. LBL method used for the formation of multi-layer GO, which is subsequently chemically reduced to yield RMGO electrodes. The quartz substrate is first charged by dipping into a PEI solution and subsequently dipped into the GO solution. The controlled dipping and rinsing process is repeated three times to form a GO film. Following the reduction of the GO film, RMGO films with 10 nm thickness are formed (as observed by AFM, see Figure S4c and S5 below). Pictorial images of the GO film and the RMGO are shown in Figure 2d (main text).
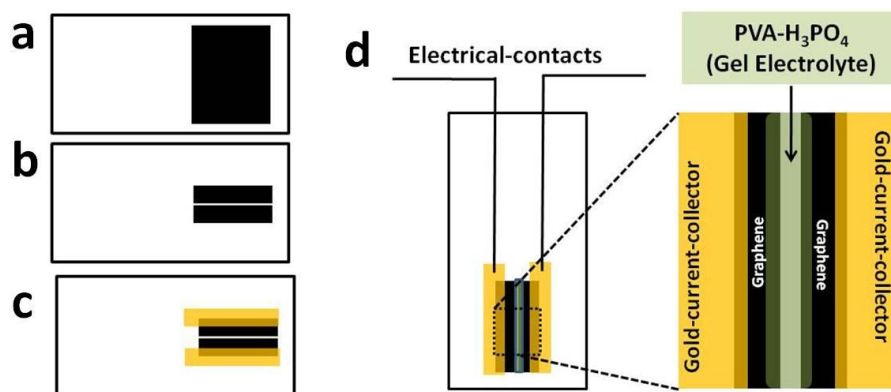

Figure S3. The various stages of "in-plane" 2D graphene device fabrication are illustrated in the order in which the device was prepared. A typical graphene film (this can be either G or RMGO) is shown in (a). After defining the active area of the total graphene material to be utilized as the electrode physically a gap is created using a razor sharp blade (b). Typically, the gaps created are ~60 μm. The active area of the electrode is then covered using a home-made mask and then gold (current collector) is sputtered to provide electrical contacts (c). Finally, the polymer-gel electrolyte is deposited selectively over the gap and the pre-defined graphene electrode area and allowed to dry (d).
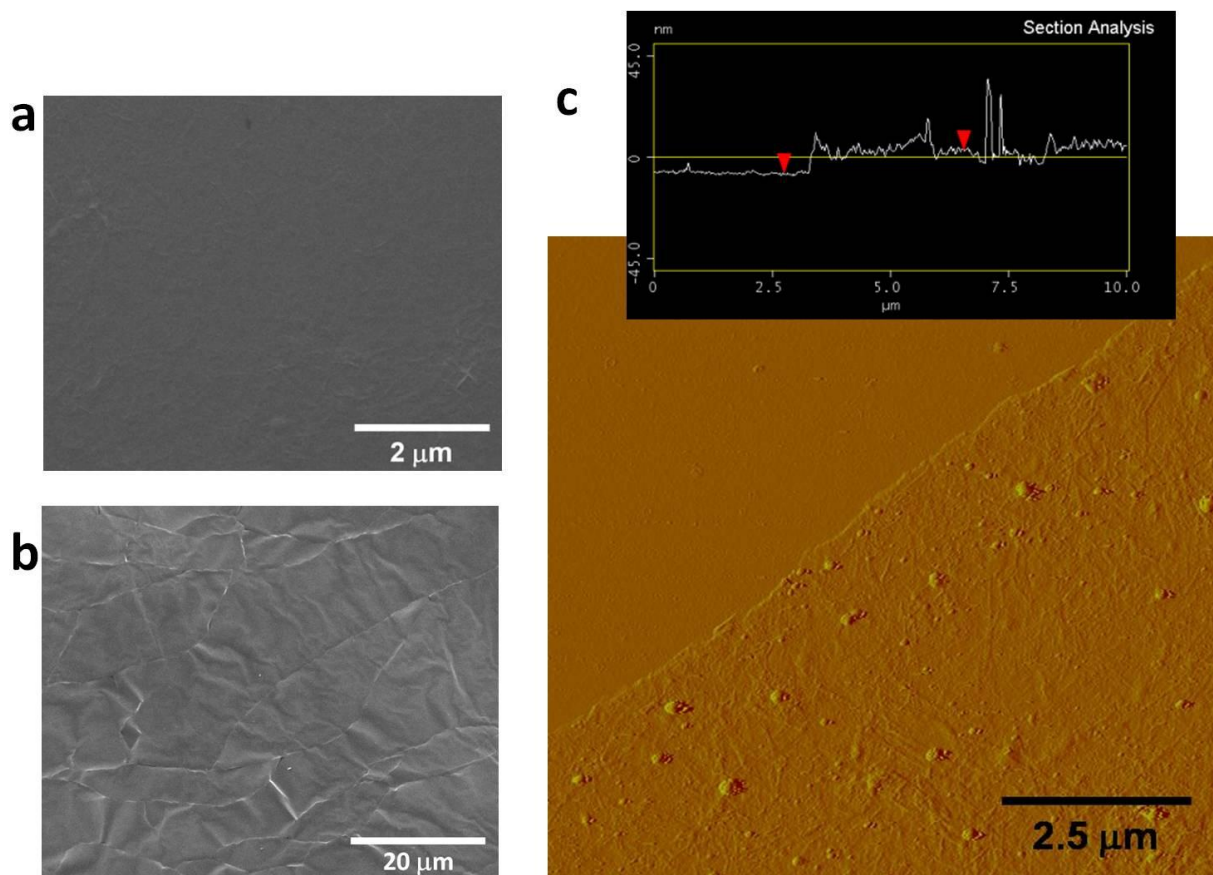
Figure S4. (a) SEM image of the RMGO films as formed after LBL and subsequent chemical reduction. Very smooth films over large scale-lengths could be observed. This fact is further confirmed by AFM analysis. (b) SEM image of inner layers of the RMGO film after cleaving the top surface using scotch tape. It is clear that stacked layers with continuous contact leading to uniform films are indeed formed by the layer-by-layer method. (c) A representative AFM image of the RMGO film along with the line-scan analysis showing a 10 nm film thickness. From several AFM line-scan measurements over different regions of the RMGO films a 10 nm thickness is apparent. Additionally, the 10 nm height profiles were obtained by using depth profile analysis on several different regions in the RMGO (see **Figure S5**). For the AFM analysis the RMGO films were transferred from quartz substrate to freshly cleaved atomically flat mica surface.
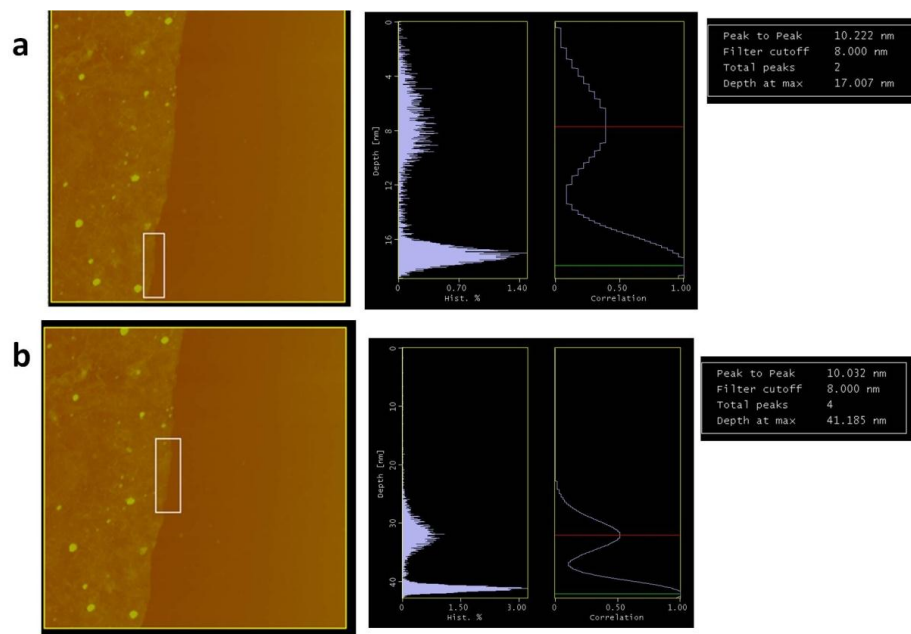
Figure S5. AFM depth profiles of RMGO films on mica substrate. Two different regions within the same area of the RMGO films were subjected to the depth profile analysis using the DI Nanoscope IIIa software. The peak to peak fit analysis over different regions reveals a 10 nm thickness. These results are similar to those observed by the line-scan analysis.
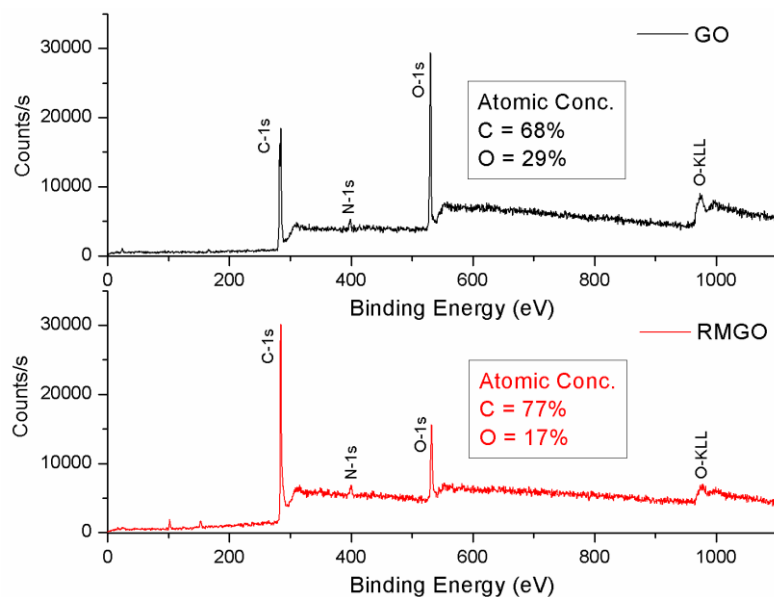

Figure S6. XPS profiles for the GO films (top) obtained by LBL method and the RMGO films (bottom) obtained by subsequent chemical reduction of the GO films. Upon reduction of the GO films using hydrazine a remarkable reduction in the atomic concentrations of oxygen and subsequent increase in the carbon implies that the reduction of the GO films has indeed occurred.
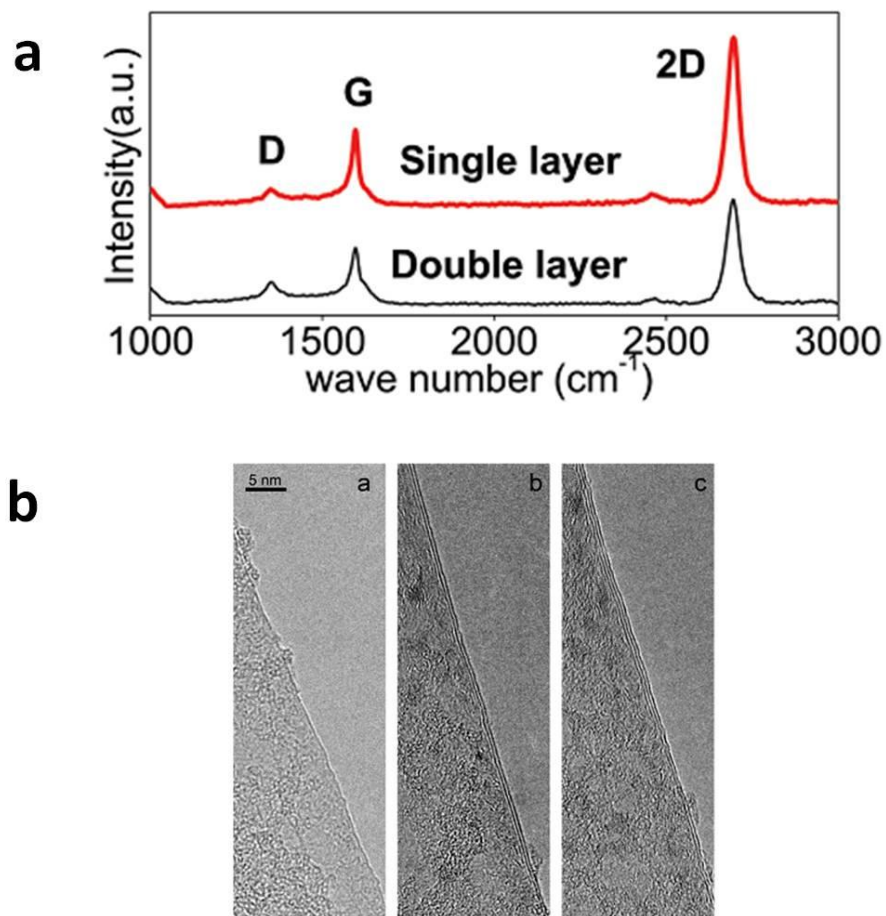
Figure S7. Raman spectra obtained from different regions of the pristine graphene film grown using CVD method (a)[1]. The presence of small amounts of defect is indicated by the trace amounts of D peaks. Furthermore, appearance of sharp G peak and its ratio with the more intense 2D peak implies high quality graphene has been synthesized using the CVD method. These graphene films show single-layer features in more than 90% of the regions. However, in very few regions small amounts of double and triple layer graphene are evident from both Raman and TEM measurements. A representative TEM images showing edge structures with one, two and three layers are shown in (b).
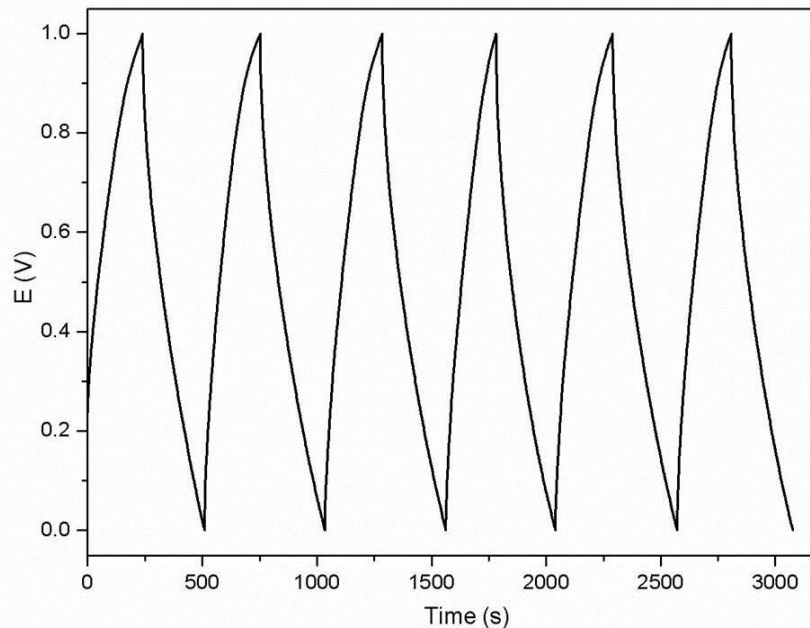
Figure S8. The charge-discharge curves for the pristine graphene measured at constant current density of 630 mAcm^{-2}.

3) Reasoning for a 10 nm RMGO film.

The key reason for the growth of the 10 nm RMGO film is the measurable mass associated with it. RMGO films thinner than 10 nm had negligible weight and therefore obscure gravimetric consideration of the figures of merit. Though arguably, G is much lighter and also precludes the measurements of the weights, the fact that G has a more well-defined structure than RMGO allows for theoretical estimation of weight. However, as will be discussed below it is more convenient to base our quantitative analysis using geometrical area considerations rather than gravimetric normalization as will become evident below.

4) Calculations for the figures of merit for G.

From the impedance measurements (EIS) an internal resistance values corresponding to 77 kΩ for RMGO and 747 kΩ for the G was determined. Using these internal resistance values energy and peak power densities for the RMGO and G films were calculated. We account for only the geometrical area in case of G films for evaluating the energy and peak power density.

2) Energy Density (per geometrical area) = $0.5CV^2/A$ = 10 μW.s.cm^{-2} = 2.8 nWhcm^{-2}

3) Power Density (per geometrical area) = $V^2/(4R_{ESR}*A)$= 2 μWcm^{-2}

For the RMGO films energy and peak power densities were calculated to be 8.5 Whkg^{-1} and 5.7 kWkg^{-1}, respectively. In terms of the geometrical area, the above mentioned gravimetric values correspond to energy density of 14 nWhcm^{-2} and peak power density of 9 μWcm^{-2}. **Table S1** summarizes the overall evaluations of energy and peak power density.

Table S1. Overall evaluation of energy density and power density

Mater.	Energy Density		Power Density	
	WhKg^{-1}	nWhcm^{-2}	kWKg^{-1}	μWcm^{-2}
SG	-	2.8	-	2
RMGO	8.5	14	5.7	9

5) Stacked Vs 'In-plane' device

In order to compare the performance for the same area of the electrodes, with similar amounts of the electrolyte stacked devices using the multi-layer graphene electrodes were created as shown in Figure S9.
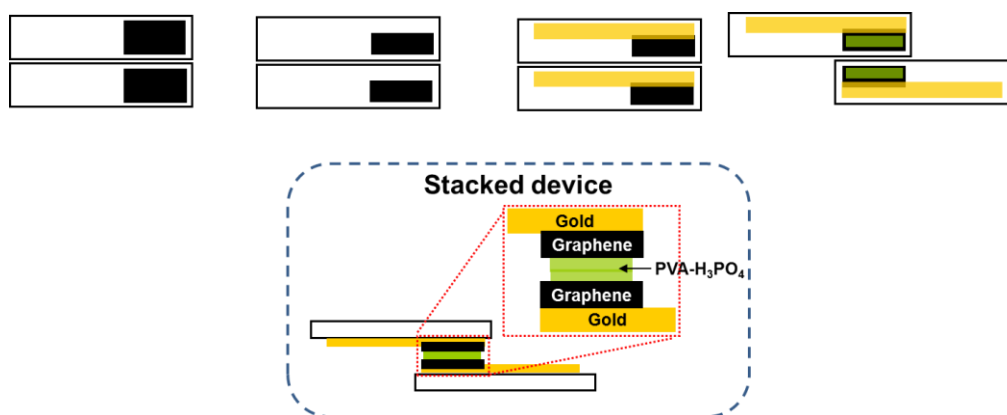

Figure S9. Schematic rendering of the steps involved in the fabrication of stacked (conventional) electrodes based on multi-layer graphene. Two separate quartz slides were utilized to create the initial large scale RMGO electrodes by the LBL method (same as the one used for 'in-plane' devices). After cropping off the film to the desired size, the polymer-gel electrolyte was applied onto both the electrodes and was allowed to dry overnight. After this the two separate electrodes with the dried electrolytes were sandwiched together by applying a small weight from the top to ensure full contact. The devices were then tested for their characteristic performance. The resulting performance and its comparison to those of the in-plane geometry is shown in Table S2.

Table S2. Comparison of the specific capacity for the stacked Vs In-plane device geometry for the RMGO electrodes with ~ 10 nm thickness.

Geometry	Stacked (μFcm^{-2})	In-plane (μFcm^{-2})
RMGO	140	394

Reference (Supplementary)

(1) Srivastava, A.; Galande, C.; Ci, L.; Song, L.; Rai, C.; Jariwala, D.; Kelly, K. F.; Ajayan, P. M. *Chem. Mater.* **2010**, *22*, 3457.
(2) Kaempgen, M.; Chan, C. K.; Ma, J.; Cui, Y.; Gruner, G. *Nano Lett.* **2009**, *9*, 1872.